Chemical Science



EDGE ARTICLE

View Article Online



Cite this: Chem. Sci., 2025, 16, 16751

d All publication charges for this article have been paid for by the Royal Society of Chemistry

Received 6th June 2025 Accepted 1st August 2025

DOI: 10.1039/d5sc04122h

rsc.li/chemical-science

Multinuclear Cu_nS_m clusters encapsulated by aromatic micelles as aqueous red-to-NIR phosphorescent ink

Kazuki Toyama, D Yuya Tanaka D * and Michito Yoshizawa D *

Sulfur-bridged copper clusters are important biocomponents, yet their artificial analogues have rarely been studied in solution due to poor solubility and stability. Here we report the preparation of red-to-nearinfrared (NIR) phosphorescent solutions from multinuclear Cu_nS_m clusters upon encapsulation by aromatic micelles in water. For instance, whereas a 2-mercapto-6-methylpyridine-based Cu₆S₆ cluster shows no solution-state emission owing to its insolubility in common solvents, the encapsulated cluster emits strong red-to-NIR phosphorescence ($\Phi = 34\%$; $\lambda = 550-850$ nm) with high stability, even under aerobic and ambient conditions. Similar host-quest complexes are also obtained from analogous Cu₆S₆ clusters, displaying substituent-dependent red-to-NIR emission in water. The present method is applicable to larger Cu₁₂S₆ and smaller Cu₄I₄ clusters to generate aqueous, red, yellow, and green emissive solutions. Notably, the resultant host-quest solution can be used as aqueous colorless ink, for potential security applications, which exhibits strong emission when painted on paper in the red-to-NIR region upon UV-light irradiation.

Introduction

Multinuclear metal clusters embedding heteroatoms exhibit varied structures with intriguing physicochemical properties, which cannot be found in related clusters without heteroatoms as well as mononuclear metal complexes.1 For instance, sulfurbridged metal clusters, composed of Fe_nS_m and Cu_nS_m cores (e.g., n = 2-8 and m = 1-8), have been known as key biocomponents with unique redox ability, protected in protein cavities (Fig. 1a). Synthetic multinuclear Cu_nS_m clusters have also attracted interest, due to their characteristic photophysical properties and reactivities with tunability.1,3 However, except for biological systems, the majority of such artificial Cu_nS_m clusters are insoluble in water-organic solvent mixtures as well as water, which interferes with their green chemical processes and biomedical applications.4 The intrinsic instability of the Cu-S bonds in solution also restricts their usability. To overcome these drawbacks, water-soluble multinuclear clusters have been generally prepared by utilizing hydrophilic thiol-based ligands attached covalently (Fig. 1b)5 and by encapsulation in alkylbased micelles (Fig. 1c).6 Since these usual methods are inapplicable to Cu_nS_m clusters, owing to the facile oxidation/ reduction of the Cu(1) moieties, 4b,10c their water-solubilization and resultant solution-state strong emission remain elusive so far. To expand Cu_nS_m-based cluster chemistry in water by a new

Laboratory for Chemistry and Life Science, Institute of Integrated Research, Institute of Science Tokyo, 4259 Nagatsuta, Midori-ku, Yokohama 226-8501, Japan. E-mail: yoshizawa.m.ac@m.titech.ac.jp; ytanaka@res.titech.ac.jp

method, we herein report (i) the facile preparation of aqueous solutions of Cu₆S₆ clusters upon encapsulation by aromatic micelles (Fig. 1d). (ii) The obtained host-guest solutions display strong red-to-near-infrared (NIR) phosphorescence (up to $\Phi = 34\%$) with high stability under ambient conditions. (iii) Similarly, various host-guest complexes are prepared using analogous Cu₆S₆ clusters, showing wide red-to-NIR emission

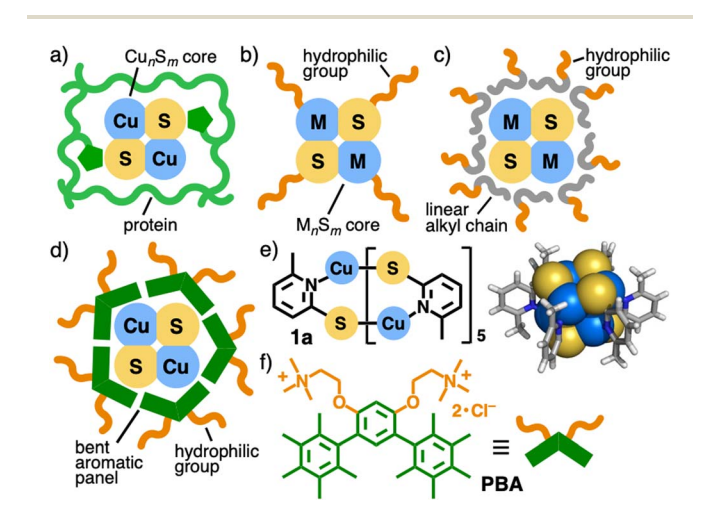


Fig. 1 Preparation of aqueous Cu_nS_m or M_nS_m cluster-based solutions, using (a) a protein cavity, (b) hydrophilic thiol ligands and (c) an alkyl micelle (except for M = Cu), and (d) an aromatic micelle (M = Cu; this work). (e) Cu_6S_6 cluster 1a and its crystal structure. 14,15 (f) Bent aromatic amphiphile PBA.

depending on the substituents. (iv) This method enables other multicopper clusters, with a $\mathrm{Cu_{12}S_6}$ and $\mathrm{Cu_4I_4}$ core, to generate red, yellow, and green emissive complexes in water. Furthermore, (v) the obtained host–guest solution can be used as redto-NIR phosphorescent ink on paper without visible color under room light, for potential security applications.

Unlike multicopper clusters without heteroatoms, Cu_nS_m clusters show strong phosphorescent emission in the solid state, whereas this feature is lost to a large extent in solution. 14,4,8 Mercaptopyridine-based Cu₆S₆ clusters (e.g., Fig. 1e), as a representative example, are poorly soluble in common organic solvents as well as insoluble in water, without laborious functionalization. Larger Cu₁₂S₆ clusters with bisphosphine ligands10 are soluble in organic solvents yet suffer from thermal instability and air-sensitivity. For the efficient encapsulation of such multicopper clusters with dimensions of 1-2 nm, here we employed bent aromatic amphiphile PBA, bearing two pentamethylbenzene panels and two trimethylammonium groups (Fig. 1f).11,12 Its spontaneous and quantitative assembly generates aromatic micelle (PBA)_n ($n = \sim 5$) in water at room temperature. Thanks to the hydrophobic effect and multiple CH- π interactions in the adaptable cavity, the aromatic micelle displays wide-ranging host ability toward planar and large aromatic compounds as well as metal-complexes with adequate stability,11,13 unlike conventional alkyl micelles. On the other hand, like other host compounds reported previously,7 its encapsulation ability toward sterically demanding, multinuclear M_n clusters (n > 3) with low solution-state stability has not been revealed to date.

Results and discussion

Encapsulation of multinuclear Cu₆S₆ clusters by aromatic micelles

Bent aromatic amphiphile PBA displayed superior encapsulation ability toward 2-mercapto-6-methylpyridine-based Cu₆S₆ cluster 1a in water, as compared with typical alkyl amphiphiles. Colorless solid PBA (0.7 mg, 1.0 µmol) and pale yellow solid 1a (0.6 mg, 0.5 µmol) were ground with a mortar and pestle for 1 min.¹⁴ Water addition (1.0 mL) to the mixture, centrifugation, and filtration gave rise to a clear colorless solution including $(\mathbf{PBA})_n \cdot (\mathbf{1a})_m$ in a nearly quantitative manner based on \mathbf{PBA} (Fig. 2a). The UV-visible spectrum showed new shoulder bands at 300-420 nm, besides a prominent band for PBA (250-300 nm), which indicates the successful water-solubilization of $(1a)_m$ upon encapsulation (Fig. 2b). The absorption bands of $(1a)_m$ within $(PBA)_n$ were significantly blue-shifted $(\Delta \lambda)$ \sim 130 nm), as compared to that of solid 1a, suggesting the suppression of cluster aggregation and the isolation of a single cluster. The obtained, aqueous host-guest solution is stable enough under ambient conditions (i.e., room temperature and light) for >1 week (Fig. 6c and S27b), as discussed later and at elevated temperature (e.g., 80 °C; Fig. S27c). The concentration of 1a solubilized in H2O upon encapsulation was calculated to be 0.1 mM by UV-visible and ICP-AES studies (1.0 mM based on PBA; Fig. S29). The core size and composition of the product were estimated to be 2.6 nm and 10:1 PBA/1a, respectively, by

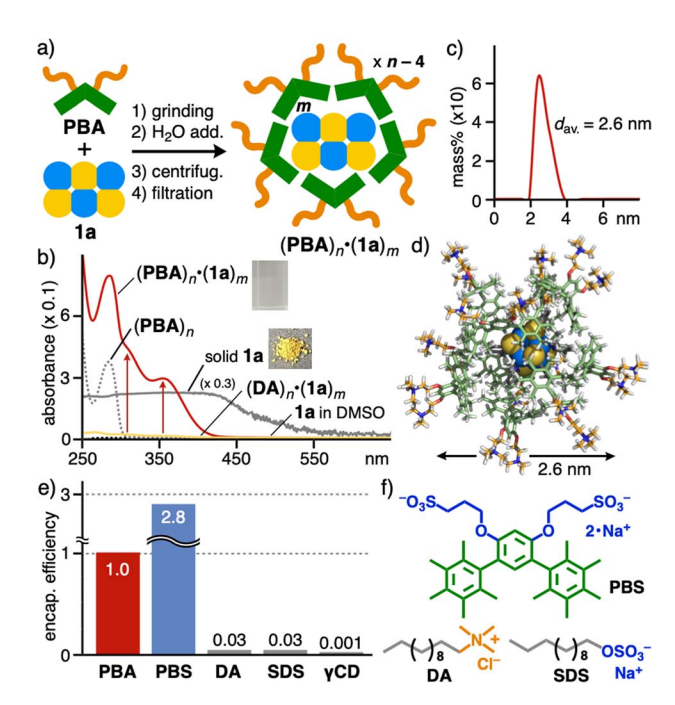


Fig. 2 (a) Preparation of an aqueous solution of the host–guest complex (PBA) $_n$ ·(1a) $_m$. (b) UV-visible spectra (H $_2$ O, r.t., 1.0 mM based on PBA) of (PBA) $_n$ ·(1a) $_m$. (DA) $_n$ ·(1a) $_m$, and (PBA) $_n$ in H $_2$ O, 1a in DMSO (<10 $_{\mu}$ M, saturated), and solid 1a. (c) DLS chart (H $_2$ O, r.t.) of (PBA) $_n$ ·(1a) $_m$ · (d) Optimized structure of (PBA) $_1$ ·1a. (e) Relative encapsulation efficiency of various amphiphiles and $_{\gamma}$ CD toward 1a in water. (f) Aromatic and alkyl amphiphiles studied herein.

the DLS (Fig. 2c) and UV-visible analyses (Fig. S29). On the basis of these experimental results and the crystal structure of $\mathbf{1a}$, molecular modeling studies indicated the formation of $(\mathbf{PBA})_{10} \cdot \mathbf{1a}$, with a core diameter of 2.6 nm, as the major product (Fig. 2d). The present efficient encapsulation most probably stems from the hydrophobic effect and multiple CH– π interactions between **PBA** and **1a**.

To compare encapsulation efficiency, alkyl amphiphiles **DA** and **SDS**, bent aromatic amphiphile **PBS** with anionic hydrophilic groups (Fig. 2f), and γ -cyclodextrin (γ CD)¹⁶ were employed under the same conditions. From the UV-visible spectra of the resultant host–guest complexes (Fig. S20), the cluster-based band intensities ($\lambda=353$ nm) revealed low efficiencies with dodecyltrimethylammonium chloride (**DA**), sodium dodecyl sulfate (**SDS**), and γ CD (<0.03-fold) yet high efficiency with **PBS** (2.8-fold), relative to that of **PBA** (Fig. 2e). These results revealed the unusability of the conventional micellar and tubular hosts as well as supported the importance of host–guest CH– π interactions for the efficient preparation of the **1a**-based host–guest solution.

Strong emission of aqueous host-guest complexes

The aqueous host-guest solution of $(PBA)_n \cdot (1a)_m$ in hand showed the strongest emission under ambient conditions, among the tested host-guest solutions. No solution-state emission was detected from 1a in any common solvents (e.g., DMSO and CH_2Cl_2 ; Fig. 3a, c, and S22a), owing to its

Edge Article

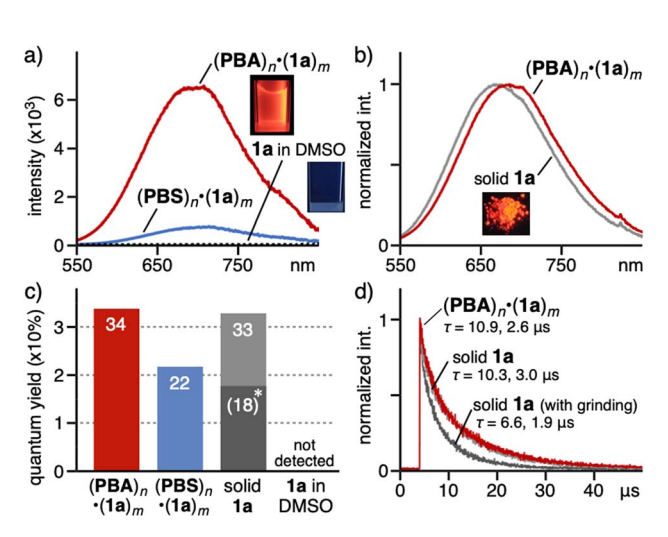


Fig. 3 (a) Emission spectra (r.t., $\lambda_{\rm ex}=320$ nm, 1.0 mM based on amphiphiles) of (PBA or PBS) $_n$ · (1a) $_m$ in H $_2$ O and 1a in DMSO (<10 μ M, saturated), and (b) the comparison with that of solid 1a. (c) Emission quantum yields (H $_2$ O, $\lambda_{\rm ex}=320$ nm) of (PBA or PBS) $_n$ · (1a) $_m$, solid 1a (*: after grinding), and 1a in DMSO. (d) Emission lifetimes ($\lambda_{\rm ex}=340$ nm) of (PBA) $_n$ · (1a) $_m$ in H $_2$ O ($\lambda_{\rm det}=685$ nm) and solid 1a (with/without grinding, $\lambda_{\rm det}=695/670$ nm).

insolubility. In contrast, the solution of $(PBA)_n \cdot (1a)_m$ displayed intense red emission, derived from the triplet-state cluster center, with a broad band at $\lambda_{\text{max}} = 685 \text{ nm}$ and a quantum yield (Φ) of 34% upon light irradiation at 320 nm, under aerobic conditions.14 Under the same conditions, anionic derivative $(PBS)_n \cdot (1a)_m$ also showed red emission with slightly lower efficiency ($\Phi = 22\%$), most probably owing to side chain-induced photo deactivation. Nearly no band was observed in the emission spectrum of $(\gamma CD)_n \cdot (1a)_m$ in water (Fig. S20), ¹⁴ due to the poor uptake efficiency. The emission band of $(PBA)_n \cdot (1a)_m$ in water was slightly red-shifted ($\Delta \lambda_{\rm em} = +15$ nm) relative to that of solid 1a (Fig. 3b), in contrast to their absorption bands (Fig. 2b). Remarkably, the emission efficiency is comparable to that of solid **1a** ($\Phi = 33\%$) yet much higher than that of ground solid **1a** ($\Phi = 18\%$; Fig. 3c and S24),^{14,17} even including the grinding process. The emission lifetime analysis of $(PBA)_n \cdot (1a)_m$ in water elucidated its phosphorescence ($\tau = 10.9$ and 2.6 µs; Fig. 3d), which is usually largely quenched under aerobic conditions. The lifetime is slightly longer than that of solid $\mathbf{1a}$ ($\tau = 10.3$ μs).18 These experimental and theoretical structural analyses (Fig. 2d) indicated that the present unusual results are mainly derived from the host-based steric shielding effect against oxygen through tight host-guest interactions.

Aqueous host–guest solutions were prepared from Cu₆S₆ clusters **1b–e** and **1f** with various substituents (*i.e.*, R = H, CH₃, Br, and CF₃) at the 5-position and quinoline rings, respectively (Fig. 4a). In the same manner as (**PBA**)_n·(**1a**)_m, the grinding and filtration protocol using solids **PBA** (2.0 μ mol), **1b–f** (1.0 μ mol), and H₂O (2.0 μ m) led to the formation of host–guest complexes (**PBA**)_n·(**1b–e**)_m and (**PBA**)_n·(**1f**)_m as colorless and pale yellow aqueous solutions, respectively. The UV-visible spectra of the resultant solutions showed new shoulder bands at 300–420 nm for bound **1b–e** and a new broad band at $\lambda_{max} = 395$ nm for

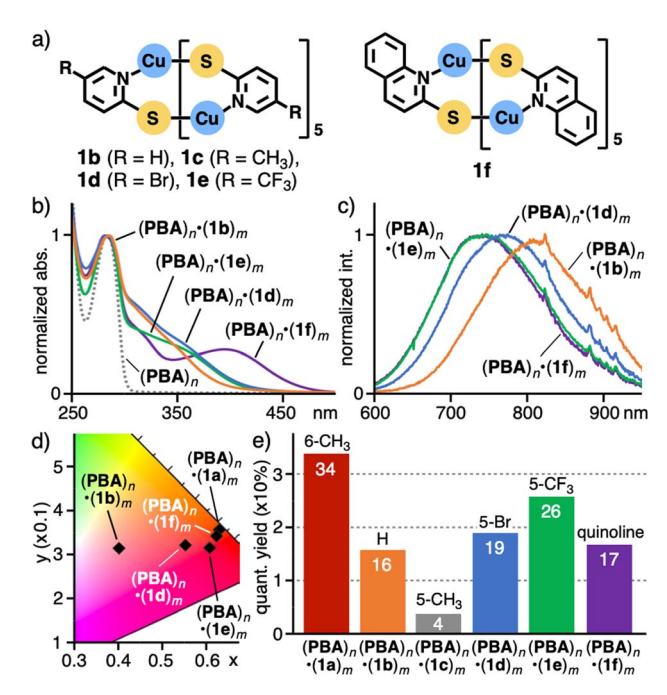


Fig. 4 (a) Cu_6S_6 clusters ${\bf 1b-f}$ with various substituents. (b) UV-visible spectra (H_2O , r.t., 1.0 mM based on PBA) of host–guest complexes (PBA) $_n$ ·(${\bf 1b-f}$) $_m$ and (c) their emission spectra ($\lambda_{\rm ex}=320$ nm). (d) CIE diagram (H_2O , r.t., $\lambda_{\rm ex}=320$ nm) of (PBA) $_n$ ·(${\bf 1a-f}$) $_m$ in water and (e) their emission quantum yields.

bound 1f (Fig. 4b), which confirmed the successful watersolubilization of $(1b-f)_m$ upon encapsulation. Emission spectra of complexes $(PBA)_n \cdot (1b-f)_m$ in water were red-shifted $(\Delta \lambda_{\rm em} = +55 \text{ to } +120 \text{ nm})$, relative to that of $(PBA)_n \cdot (1a)_m$ (Fig. 4c), due to reduced steric hindrance between the cluster ligands, as suggested by DFT calculation (Fig. S50).18 In particular, non-substituted $(\mathbf{PBA})_n \cdot (\mathbf{1b})_m$ $(\mathbf{R} = \mathbf{H})$ showed the largest shifted red-to-NIR emission at 805 nm ($\Delta \lambda_{em} = +120$ nm) among the tested complexes. The emission quantum yields of hostguest complexes $(PBA)_n$ including clusters **1b-f** were moderate (16-26% except for 1c (4%); Fig. 4e) and their emission color was widely tunable depending on the small substituents (Fig. 4d and S18). These yields were again higher than those of ground solids 1b-f without PBA (1.1 to 17-fold; Fig. S24 and S25), because of the loss of their crystallinity and the generation of undesired intermolecular contact in the solids.

Efficient emission and stabilization of larger and smaller multinuclear clusters within aromatic micelles

Larger/smaller multinuclear clusters such as Cu_{12}S_6 cluster 2 with four bis(diphenylphosphino)pentane ligands and Cu_4I_4 clusters 3a and 3b (Fig. 5a) were encapsulated by aromatic micelles in water and the resultant aqueous solutions emitted moderate red and strong yellow/green phosphorescence, respectively. In a similar manner to $(\text{PBA})_n \cdot (\text{1a})_m$, host-guest complex $(\text{PBA})_n \cdot (2)_m$ was obtained as a nearly colorless aqueous solution, using PBA (2.0 µmol), 2 (0.3 µmol), and H₂O (2.0 mL), in an optimized ratio. The UV-visible and emission spectra showed a new broadened shoulder band (300–500 nm; Fig. 5b)

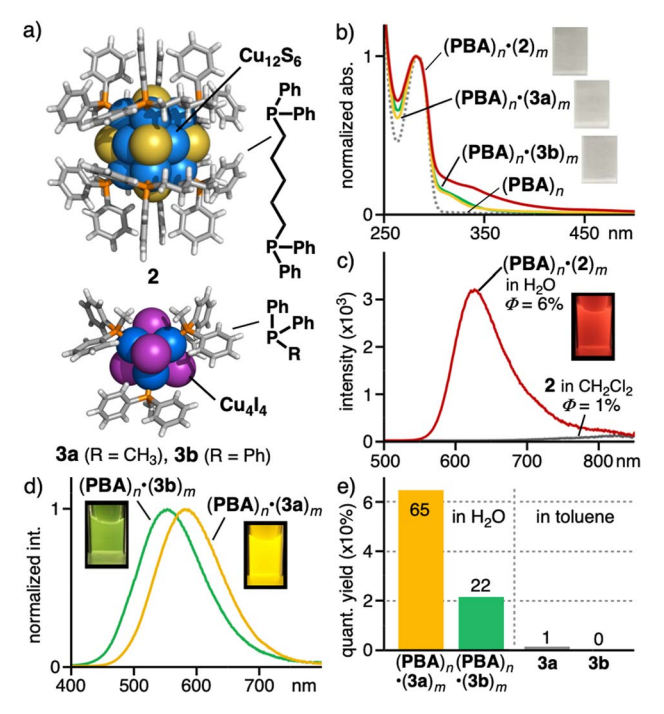


Fig. 5 (a) $Cu_{12}S_6$ cluster 2 and Cu_4I_4 clusters 3a and 3b. (b) UV-visible spectra (H₂O, r.t., 1.0 mM based on PBA) of (PBA)_n, (PBA)_n · (2)_m, and $(PBA)_n \cdot (3a \text{ or } 3b)_m$. (c) Emission spectra (r.t., $\lambda_{ex} = 320 \text{ nm}$, 1.0 mM based on PBA) of $(PBA)_n \cdot (2)_m$ in H_2O and 2 in CH_2Cl_2 (<0.1 mM, saturated). (d) Emission spectra (H_2O , r.t., $\lambda_{ex} = 320$ nm, 1.0 mM based on PBA) of $(PBA)_n \cdot (3a \text{ or } 3b)_m$ and (e) their emission quantum yields ($\lambda_{ex} = 320$ nm; **3a** and **3b** in toluene (0.1 mM)).

and a relatively sharp band ($\lambda_{max} = 625$ nm, $\Phi = 6\%$; Fig. 5c), respectively, attributed to bound cluster 2. In contrast, the solution of 2 in CH₂Cl₂ showed a very weak emission band (λ_{em} = >650 nm, Φ = 1%; Fig. 5c), derived from its decomposed clusters through aerobic oxidation. 10a,c,19 Colorless aqueous solutions of host-guest complexes $(PBA)_n \cdot (3a)_m$ $(\mathbf{PBA})_n \cdot (\mathbf{3b})_m$ were also obtained by the treatment of **PBA** with 3a bearing four methyldiphenylphosphines or 3b bearing four triphenylphosphines, 14,20 in a manner similar to the preparation of $(PBA)_n \cdot (2)_m$. These solutions displayed strong yellow emission ($\lambda_{\rm max} = 580$ nm, $\Phi = 65\%$) and moderate green one ($\lambda_{\rm max} =$ 550 nm, $\Phi = 22\%$), respectively (Fig. 5d and 5e), while their absorption spectra were comparable (Fig. 5b). The high quantum yield most likely stems from the steric restriction of the ligand rotation on 3a within (PBA)_n (Fig. S41).¹⁴ Whereas clusters 3a and 3b are soluble in toluene (Fig. S38a and S38b), the resultant solutions provided quite poor emission properties under aerobic conditions (e.g., $\Phi = 0$ -1%; Fig. 5e, S38a and S38b), in sharp contrast to their host-guest complexes.²¹ Within the aromatic micelles in solution, thus, the cluster structures of 2 and 3a and 3b were effectively stabilized against air and nonradiative relaxation, respectively (Fig. S33 and S37),14,22 again due to the host-based shielding effect.

Applications as security ink

Host-guest complex $(PBA)_n \cdot (1a)_m$ in hand showed a potential application as security ink to realize anti-counterfeiting.23 Like the

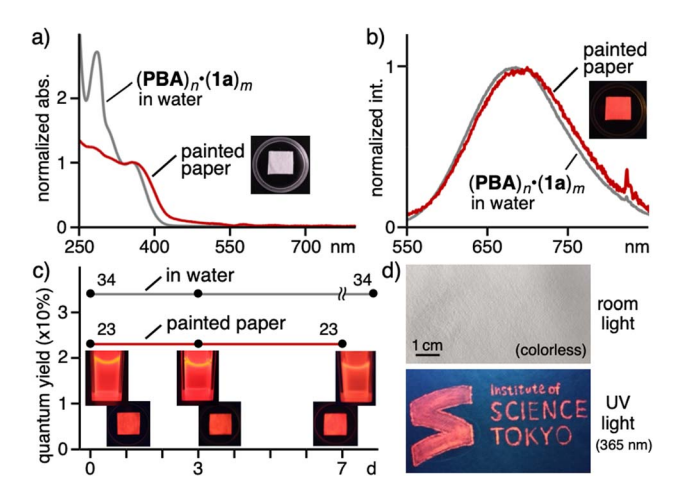


Fig. 6 (a) UV-visible and (b) emission spectra (r.t., 1.0 mM based on PBA, $\lambda_{\rm ex}=320$ nm) of (PBA)_n·(1a)_m painted on paper and in H₂O. (c) Time-dependent, emission quantum yields (r.t., 1.0 mM based on PBA, $\lambda_{\rm ex}=320$ nm) of (PBA) $_n\cdot(1a)_m$ in H₂O (undegassed) and painted on paper (stored in N₂). (d) Photographs of a university logo and name, drawn with an aqueous $(PBA)_n \cdot (1a)_m$ solution, taken under room light (top) and UV light (365 nm, bottom).

aqueous solution, its painting on paper (i.e., cellulose filter paper) was colorless under room light, only with a weak absorption band in the visible region in the UV-visible diffuse reflectance spectrum (Fig. 6a). In contrast, the painted paper displayed red-to-NIR emission with strong intensity ($\Phi = 23\%$) upon UV-light irradiation under ambient conditions ($\lambda_{ex} = 320$ nm, Fig. 6b). An emission band was clearly observed in the red-to-NIR region (λ_{max} = 700 nm) from the paper in the spectrum, which is comparable to that of $(PBA)_n \cdot (1a)_m$ in water. The present ink provides several advantages: (i) environmentally benign water can be used as the solvent and the host-guest solution is odorless, (ii) the aggregation-caused visible absorption (<560 nm) from solid 1a is fully suppressed upon encapsulation, (iii) the small particle size $(\sim 3 \text{ nm})$ excludes light scattering on the paper, which interferes with invisibility, (iv) the red-to-NIR emission from the solution remains intact (~100% retention), without any visible coloration, even after standing for more than 1 week (at least 10 d) even under ambient, aerobic conditions (Fig. 6c and S27b), (v) the emissivity of the painted paper is also maintained virtually (~100% retention) after 1 week under anaerobic conditions (Fig. 6c)²⁴ and after 10 min at elevated temperature (*i.e.*, 80 °C; Fig. S44c), and (vi) after washing with organic solvents (i.e., methanol), the red-to-NIR emission is fully retained (\sim 100%; Fig. S45 and S46a).24 Accordingly, names and logos could be facilely drawn on paper (Fig. 6d). The potential security inks with red-to-NIR emission and large Stokes shifts ($\Delta \lambda > 340 \text{ nm}$) are rare so far, without the use of rare-earth elements and noble metals (e.g., Nd, Yb, Ir, and Pt).25

Conclusions

We have accomplished the preparation of aqueous red-to-NIR phosphorescent solutions of multinuclear Cu_nS_m clusters upon facile encapsulation for the first time. Once **Edge Article Chemical Science**

mercaptopyridine-based Cu₆S₆ clusters, which hardly emit by themselves in solution, were encapsulated by aromatic micelles in water, the resultant host-guest solutions exhibited strong red-to-NIR phosphorescent emission. Unlike previously reported aliphatic micelles as well as coordination cages, the present micelle efficiently encapsulated various multinuclear clusters, such as Cu₁₂S₆ and Cu₄I₄ clusters, generating aqueous phosphorescent solutions with various emission colors. Colorless yet strong red-to-NIR emissive features, besides high water, air, and thermal stability as well as large scale synthesis, established the present host-guest solutions as potential security ink. Further preparation of multinuclear cluster-based solutions (e.g., large heteronuclear Au, Mn, and Pt clusters) via this encapsulation strategy would provide new materials and catalytic applications in water.

Author contributions

K. T., Y. T., and M. Y. designed the work, carried out the research, analyzed the data, and wrote the paper. M. Y. is the principal investigator. All authors discussed the results and commented on the manuscript.

Conflicts of interest

There are no conflicts to declare.

Data availability

CCDC 2420528 and 2420529 contain the supplementary crystallographic data for this paper.15

The experimental procedures and analytical data are available in the SI. See DOI: https://doi.org/10.1039/d5sc04122h.

Acknowledgements

This work was supported by JSPS KAKENHI (Grant No. JP22H00348/JP23K17913/JP25K01783). PXRD measurements were performed with the help of Hiroto Toyoda and Prof. Toshiyuki Yokoi (Science Tokyo). K. T. acknowledges JST SPRING (Grant No. JPMJSP2106) and JSPS Research Fellowship for Young Scientists (Grant No. 25KJ1257). The theoretical calculations were performed using computers in the Research Center for Computational Science, Okazaki, Japan (24-IMS-C060 and 25-IMS-C062).

Notes and references

- 1 (a) V. W.-W. Yam and K. K.-W. Lo, Chem. Soc. Rev., 1999, 28, 323–334; (b) O. Fuhr, S. Dehnen and D. Fenske, Chem. Soc. Rev., 2013, 42, 1871-1906; (c) R. Jin, C. Zeng, M. Zhou and Y. Chen, Chem. Rev., 2016, 116, 10346-10413; (d) M. D. Pluth and Z. J. Tonzetich, Chem. Soc. Rev., 2020, 49,
- 2 Bioclusters: (a) D. C. Johnson, D. R. Dean, A. D. Smith and M. K. Johnson, Annu. Rev. Biochem., 2005, 74, 247-281; (b)

- S. R. Pauleta, S. Dell'Acqua and I. Moura, Coord. Chem. Rev., 2013, 257, 332-349.
- 3 (a) S. Dehnen, A. Eichhöfer and D. Fenske, Eur. J. Inorg. Chem., 2002, 279-317; (b) X. Liu and D. Astruc, Coord. Chem. Rev., 2018, 359, 112-126; (c) A. Baghdasaryan and T. Bürgi, Nanoscale, 2021, 13, 6283-6340.
- 4 (a) P. C. Ford, E. Cariati and J. Bourassa, Chem. Rev., 1999, 99, 3625-3648; (b) L. L.-M. Zhang and W.-Y. Wong, Aggregate, 2023, 4, e266.
- 5 (a) R. C. Job and T. C. Bruice, Proc. Natl. Acad. Sci. U.S.A., 1975, 72, 2478-2482; (b) F. Bonomi, M. T. Werth and D. M. Kurtz Jr, Inorg. Chem., 1985, 24, 4331-4335.
- 6 (a) K. Tanaka, T. Tanaka and I. Kawafune, *Inorg. Chem.*, 1984, 23, 516-518; (b) I. Tabushi, Y. Kuroda and Y. Sasaki, Tetrahedron Lett., 1986, 27, 1187-1190.
- 7 Aqueous host compounds (recent reviews): (a) J. Murray, K. Kim, T. Ogoshi, W. Yao and B. C. Gibb, Chem. Soc. Rev., 2017, **46**, 2479–2496; (b) E. G. Percástegui, T. K. Ronson and J. R. Nitschke, Chem. Rev., 2020, 120, 13480-13544; (c) A. P. Davis, Chem. Soc. Rev., 2020, 49, 2531-2545; (d) L. Escobar and P. Ballester, Chem. Rev., 2021, 121, 2445-2514; (e) M. A. Beatty and F. Hof, Chem. Soc. Rev., 2021, 50, 4812-4832; (f) H. P. Ferguson Johns, E. E. Harrison, K. J. Stingley and M. L. Waters, Chem.-Eur. J., 2021, 27, 6620-6644; (g) H. Takezawa and M. Fujita, Bull. Chem. Soc. Ipn., 2021, 94, 2351-2369; (h) J. N. Martins, J. C. Lima and N. Basílio, *Molecules*, 2021, **26**, 106; (*i*) L. Catti, R. Sumida and M. Yoshizawa, Coord. Chem. Rev., 2022, 460, 214460; (j) H. Nie, Z. Wei, X.-L. Ni and Y. Liu, Chem. Rev., 2022, 122, 9032-9077; (k) D. Chakraborty and P. S. Mukherjee, Chem. Commun., 2022, 58, 5558-5573; (l) W.-T. Dou, C.-Y. Yang, L.-R. Hu, B. Song, T. Jin, P.-P. Jia, X. Ji, F. Zheng, H.-B. Yang and L. Xu, ACS Mater. Lett., 2023, 5, 1061–1082.
- 8 X. Kang and M. Zhu, Chem. Soc. Rev., 2019, 48, 2422-2457.
- 9 (a) S. Kitagawa, M. Munakata, H. Shimono, S. Matsuyama and H. Masuda, J. Chem. Soc., Dalton Trans., 1990, 2105-2109; (b) H. Xie, I. Kinoshita, T. Karasawa, K. Kimura, T. Nishioka, I. Akai and K. Kanemoto, J. Phys. Chem. B, 2005, **109**, 9339–9345; (c) G.-N. Liu, R.-D. Xu, J.-S. Guo, J.-L. Miao, M.-J. Zhang and C. Li, J. Mater. Chem. C, 2021, 9,8589-8595.
- 10 (a) X.-X. Yang, I. Issac, S. Lebedkin, M. Kühn, F. Weigend, D. Fenske, O. Fuhr and A. Eichhöfer, Chem. Commun., 2014, **50**, 11043–11045; (b) A. Eichhöfer, G. Buth, S. Lebedkin, M. Kühn and F. Weigend, Inorg. Chem., 2015, 54, 9413-9422; (c) M. J. Trenerry and G. A. Bailey, Nanoscale, 2024, 16, 16048-16057.
- 11 (a) Y. Okazawa, K. Kondo, M. Akita and M. Yoshizawa, Chem. Sci., 2015, 6, 5059-5062; (b) Y. Hashimoto, Y. Katagiri, Y. Tanaka and M. Yoshizawa, Chem. Sci., 2023, 14, 14211-14216.
- 12 (a) K. Kondo, A. Suzuki, M. Akita and M. Yoshizawa, Angew. Chem., Int. Ed., 2013, 52, 2308-2312; (b) M. Yoshizawa and L. Catti, Acc. Chem. Res., 2019, 52, 2392-2404; (c) M. Yoshizawa and L. Catti, Proc. Jpn. Acad., Ser. B, 2023, 99, 29-38; (d) S. Aoyama, L. Catti and M. Yoshizawa, Angew. Chem., Int. Ed., 2023, 62, e202306399; (e)

K. Toyama, Y. Tanaka and M. Yoshizawa, *Angew. Chem., Int. Ed.*, 2023, **62**, e202308331; (f) T. Yasuda, Y. Hashimoto, Y. Tanaka, D. Tauchi, M. Hasegawa, Y. Kurita, H. Kawai, Y. Tsuchido and M. Yoshizawa, *JACS Au*, 2025, **5**, 586–592; (g) S. Aoyama, L. Catti and M. Yoshizawa, *Chem*, 2025, **11**, 102616; (h) Y. Hashimoto, Y. Tanaka, S.-Y. Liu, H. Shinokubo and M. Yoshizawa, *J. Am. Chem. Soc.*, 2025, **147**, 23060–23067.

Chemical Science

- 13 Encapsulation of M_n -complexes $(n \ge 2)$: (a) Y. Wang, H. Kai, M. Ishida, S. Gokulnath, S. Mori, T. Murayama, A. Muranaka, M. Uchiyama, Y. Yasutake, S. Fukatsu, Y. Notsuka, Y. Yamaoka, M. Hanafusa, M. Yoshizawa, G. Kim, D. Kim and H. Furuta, *J. Am. Chem. Soc.*, 2020, 142, 6807–6813; (b) M. Hanafusa, Y. Tsuchida, K. Matsumoto, K. Kondo and M. Yoshizawa, *Nat. Commun.*, 2020, 11, 6061; (c) Y. Katagiri, Y. Tsuchida, Y. Matsuo and M. Yoshizawa, *J. Am. Chem. Soc.*, 2021, 143, 21492–21496.
- 14 See the SI. As a scale-up experiment, a 100 mL solution of (PBA)_n·(1a)_m in water (0.2 mM based on PBA) was also obtained by a similar grinding protocol. The photophysical properties (Fig. S28 and S49) were comparable to those of the 1 mL scale (Fig. 2b and 3a). The ICP-AES analysis of (PBA)_n·(1a)_m (0.1 mM based on PBA) also indicated the same PBA/1a ratio, with a Cu concentration of 4.09 ppm (≈ 0.01 mM of 1a). The photophysical properties of (PBA)_n·(1a)_m were less effective against its concentration, likely due to the isolation effect.
- 15 The single crystals of **1a** were obtained from the slow diffusion between an acidic acetone/H₂O solution of 2-mercapto-6-methylpyridine and an acidic CH₃OH solution of CuSO₄·5H₂O for 11 d at r.t. (Fig. S2; CCDC-2420528). ¹⁴
- 16 Encapsulation of ionic multinuclear clusters, except for Cu_nS_m clusters: M. Haouas, C. Falaise, N. Leclerc, S. Floquet and E. Cadot, *Dalton Trans.*, 2023, **52**, 13467–13481.
- 17 The cluster structure of solid-state **1a** is relatively stable in water and after grinding. PXRD analysis indicated that the

- high crystallinity of solid **1a** decreases partially through manual grinding without **PBA** (Fig. S7).
- 18 Solid **1a** ($\tau = 10.3$ and 3.0 μs) and ground solid **1a** ($\tau = 6.6$ and 1.9 μs) provided different emission lifetimes under the same conditions (Fig. 3d). The energy difference between the ground state and the lowest excited triplet state of **1b** ($\lambda = \sim 690$ nm), calculated by the DFT method, nearly agreed with the experimental emission wavelengths of **1a–f** ($\lambda = 685-805$ nm; Fig. S50). The substituent-dependent emission from **1a–f** is derived from the distortion of the cluster cores by the steric effect.
- 19 The multinuclear cluster-based emission spectrum of $(PBA)_n \cdot (2)_m$ in water was similar to that of solid 2 (Fig. S34).
- 20 (a) M. R. Churchill and F. J. Rotella, *Inorg. Chem.*, 1977, 16, 3267–3273; (b) J. C. Dyason, P. C. Healy, L. M. Engelhardt, C. Pakawatchai, V. A. Patrick, C. L. Raston and A. H. White, *J. Chem. Soc.*, *Dalton Trans.*, 1985, 831–838.
- 21 U. Melero, J.-Y. Mevellec, N. Gautier, N. Stephant, F. Massuyeau and S. Perruchas, *Chem.-Asian J.*, 2019, 14, 3166–3172.
- 22 Observed emission lifetimes in water: $(\mathbf{PBA})_n \cdot (\mathbf{2})_m$ ($\tau = 4.5$ and 1.3 µs), $(\mathbf{PBA})_n \cdot (\mathbf{3a})_m$ ($\tau = 6.9$ µs), and $(\mathbf{PBA})_n \cdot (\mathbf{3b})_m$ ($\tau = 6.9$ and 1.3 µs; Fig. S33 and S37).
- 23 A. Abdollahi, H. Roghani-Mamaqani, B. Razavi and M. Salami-Kalajahi, *ACS Nano*, 2020, **14**, 14417–14492.
- 24 The emission properties of the printed paper were insensitive to humidity (60–70% relative humidity; Fig. S46b) and soaking in water (Fig. S48) yet sensitive to oxygen, because of weakened host-guest interactions without water. No emission was detected from the CH₃OH filtrate.
- 25 NIR phosphorescence-based materials: (a) S. V. Eliseeva and J.-C. G. Bünzli, *Chem. Soc. Rev.*, 2009, 39, 189–227; (b)
 Q. Zhao, C. Huang and F. Li, *Chem. Soc. Rev.*, 2011, 40, 2508–2524; (c) H. Xiang, J. Cheng, X. Ma, X. Zhou and J. J. Chruma, *Chem. Soc. Rev.*, 2013, 42, 6128–6185.